

동축공기 수소확산화염에서 화염-와류 상호작용 및 혼합

김문기[†] · 오정석* · 최영일* · 윤영빈*

Flame-Vortex Interaction and Mixing in Turbulent Hydrogen Diffusion Flames with Coaxial Air

Munki Kim, Jeongseog Oh, Youngil Choi and Youngbin Yoon

Abstract

This study examines the effect of acoustic excitation using forced coaxial air on the flame characteristics of turbulent hydrogen nonpremixed flames. A resonance frequency was selected to acoustically excite the coaxial air jet due to its ability to effectively amplify the acoustic amplitude and reduce flame length and NO_x emissions. Acoustic excitation causes the flame length to decrease by 15 % and consequently, a 25 % reduction in EINO_x is achieved, compared to a flame without acoustic excitation. Moreover, acoustic excitation induces periodical fluctuation of the coaxial air velocity, thus resulting in slight fluctuation of the fuel velocity. From phase-lock PIV and OH PLIF measurement, the local flow properties at the flame surface were investigated under acoustic forcing. During flame-vortex interaction in the near field region, the entrainment velocity and the flame surface area increased locally near the vortex. This increase in flame surface area and entrainment velocity is believed to be a crucial factor in reducing flame length and NO_x emission in coaxial jet flames with acoustic excitation. Local flame extinction occurred frequently when subjected to an excessive strain rate, indicating that intense mass transfer of fuel and air occurs radially inward at the flame surface.

Key Words : NO_x Emission(배출지수), Resonance Frequency(고유주파수), Flame-Vortex Interaction(화염-와류 상호작용), Entrainment Velocity(유입 속도), Flame Surface Area(화염면 면적), Local Flame Extinction(국소 소멸)

1. Introduction

Mixing process of fuel and air is of significant interest in nonpremixed jet flames because the degree of mixing rate plays a crucial role in combustion performance and the corresponding pollutant emissions. One strategy for mixing enhancement is to add coaxial air into fuel stream in a form of a jet. In general, nonpremixed jet flames with coaxial air are termed “coaxial air flame”, which constitutes the configuration of a central fuel jet and a concentric coaxial air jet. In such flames, since coaxial

air induces rapid mixing and increases mixture homogeneity of fuel and air, flame length is drastically shorten due to increased combustion intensity [1-2]. Hence the characteristic time for nitrogen oxides (NO_x) formation is accordingly reduced, attaining a lower NO_x emission than that of simple jet flames without coaxial air.

As an alternative approach for enhanced mixing, large-scale, coherent vortical structures have been extensively employed in many combustion systems. In the jet mixing layer, vortex structures could be naturally originated by initial small disturbance, which is well known as the Kelvin-Helmholtz instability. Orderly organized vortical motions could also be generated by artificially imposed perturbations, utilizing acoustically, mechanically or fluidically oscillating devices. External excitations induced by these devices increase the coherence and intensity of the large-scale motions in the

[†] 서울대학교 기계항공공학부 대학원
E-mail : kimun77@snu.ac.kr

* 서울대학교 기계항공공학부 대학원

near field. In particular, acoustic excitation of jets and flames has been widely used due to easy instrumentation and the ability to separately control the forcing frequency and amplitude.

Acoustic forcing used in the present study has been applied to jet flows and flames in many manners. Mostly, acoustic pulsing from a loud speaker was used to well organize large-scale vortical structures, which was closely related to physical phenomena such as vortex formation, mixing enhancement, vortex/flame interaction [3]. Mueller and Schefer [4] performed phase-locked, PLIF measurements of OH radical in a laminar methane-air flame interacted with vortices of various sizes and strengths and their results showed that the vortex causes significant variations in the OH layer thickness. Local flame extinction has been investigated in turbulent methane jet diffusion flames interfered by the internal jet-fluid and external annulus-fluid vortices [5]. Recently, the dynamic behavior of the diffusion flame extinction and reignition during the flame-vortex interaction processes was investigated in a nitrogen-diluted hydrogen laminar diffusion flame [6].

The vortex structures facilitate to control pollutant emissions in practical combustors. Chao et al. [7], for example, found that flame lifting and acoustic forcing at frequencies higher than the natural frequencies are effective in reducing NOx emissions in partially premixed flames. Experimental results from a compact incinerator afterburner [8] showed that acoustic excitation is efficient to enhance mixing and increase the DRE (destruction and removal efficiency) for a waste surrogate.

Although the above researches about flame-vortex interactions have been investigated to a great extent, very few have focused on jet flames interacting with the vortices formed in the mixing layer between the coaxial air jet and ambient air. Hence, the objective of this paper is to describe dynamic behaviors during flame/vortex interactions in the near field of coaxial air flames, acoustically forcing the coaxial air jet. In order to investigate the effects of acoustic forcing on mixing enhancement and NOx emissions, we measured the velocity and concentration data using different imaging techniques and analyzed vortex and flame structures.

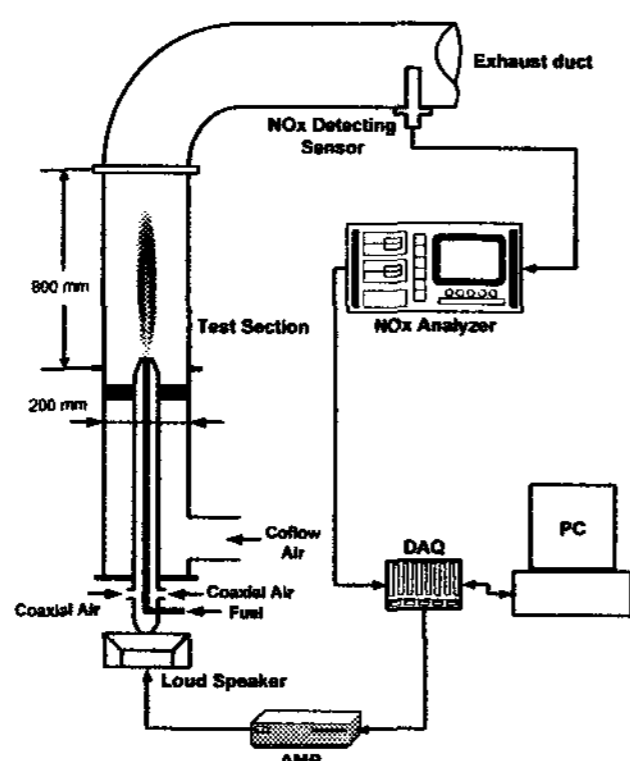


Figure 1. The schematic of experimental setup

2. Experimental Conditions and Methods

The experimental set-up consists of a flow supply section, a combustor and an exhaust gas duct as shown in Fig 1. The cross section of the combustor test-section is a 20-cm square chamber of an 80 cm in length. Nozzle geometry was composed of a fuel nozzle and a coaxial nozzle. Hydrogen was issued through the 3-mm-diameter fuel nozzle, d_F , located at the center of the combustor. The 15-mm-diameter coaxial nozzle, d_A , where coaxial air jet was injected parallel to the fuel jet was concentric to the fuel nozzle. Coflowing air was provided not only to keep the equivalence ratio constant ($\phi = 0.5$) but to maintain its velocity sufficiently low not to affect flame characteristics (<0.1 m/s).

The mass flow rate of a fuel and a coaxial air was controlled by a choked orifice. The flow conditions studied here was chosen by combining fuel jet velocity, U_F , of 175, 245, 314 m/s and coaxial air velocity, U_A , of 5, 10, 20 m/s. Honeycombs provide a homogeneous flow. A speaker driver (Sammi, 150EF), attached to the bottom of the coaxial-jet tube and driven by an amplifier with a maximum output of 150 W, was used to excite the coaxial air jet acoustically.

NOx measurements were performed using non-sampling type NOx analyzer with Zirconia-ceramic sensor (HORIBA, MEXA-720NOx). The sensor was directly inserted into the exhaust flow at 2-m downstream from the fuel nozzle, where the combustion product was found to be well-mixed with dilution air. The emission index of NOx (EINOx) was used to correct the measured emission data of NOx, where EINOx for the hydrogen non-premixed flame was defined by the total grams of NOx produced when 1kg of hydrogen is burned.

Simultaneous particle image velocimetry (PIV) and PLIF measurements were conducted for this study. For PIV measurements, seeding particles of nominally 1- μ m SiO₂ were inserted into the fuel jet and the coaxial air jet. Two 532-nm Nd:YAG lasers were operating at a frequency of 9 Hz with 100 mJ per a pulse. The laser sheets formed by cylindrical lenses were illuminated into test section and then, the scattering signals from seeding particles were recorded on a high-resolution (1008 \times 1018 pixels) Kodak ES1.0 CCD camera. The time separation between two laser pulses varies from 2 to 25 μ s according to experimental conditions. The spatial resolution is 33.6 pixels per mm and the interrogation window size is 32 pixels by 32 pixels with 50% overlap.

For OH PLIF measurements, the Q₁(6) transition of the A² Σ^+ \leftarrow X² Π ($v' = 1, v'' = 0$) band at 282.93 nm is excited by a Nd:YAG laser and a dye laser (Lumonics, HyperDYE-300). Fluorescence from the A-X(1,0) and (0,0) bands at 306~320 nm was collected with a UV-Nikkor 105m f/4.5 lens. The image is focused onto an intensified CCD camera (Princeton Instrument, PI:MAX 1K), which resolution is 1024 \times 1024 pixels with 16 bits. This camera is fitted with WG-305 and UG-11 color

glass filters to block scattering signals and the incident light of the flame. 200 images from each measurement of PIV and PLIF were phase-averaged synchronizing all the signals used here.

3. Results and Discussions

3.1 Effects of Acoustic Excitation on Flame Characteristics

The acoustic pressure at the nozzle exit of the confined combustor was measured from a microphone as random frequencies from 0 to 1,000 Hz were imposed to the bottom of the coaxial air tube. From the peak values of measured pressures, the longitudinal resonance frequencies were identified at 258, 514 and 750 Hz, which is nearly similar with the frequencies of 256.9, 523.8 and 770.6 Hz, calculated from theoretical estimation on the assumption that the schematic of the coaxial air tube is cylindrical. It has been known that the resonance frequency determined by the burner geometry is more effective to amplify the forcing amplitude and reduce NOx emissions [8]. Strongly forced acoustic excitation, however, may cause flame lift-off and blow-out [9], of which regions are of no interest because the present study is restricted to the attached flames. Thus, the resonance frequency at 514 Hz was chosen to drive the coaxial air jet acoustically, with forcing amplitude not exceeding the limit of flame lift-off and blow-out regions.

Vortex pairing formed at the side of the outer coaxial-jet has the potential to affect global properties such as flame length and NOx emissions. The visible flame length of the coaxial jet flame with acoustic excitation is considerably shorter than that of simple jet flame without coaxial air and acoustic excitation. Figure 2(a) shows the variation of normalized flame length, L_f/d_f , as a function of the coaxial air to fuel velocity ratio, U_A/U_F , in coaxial air flames with acoustic excitation compared to coaxial jet flames without acoustic excitation. Note that L_f is the visual flame length and the acoustic power of the forcing frequency, $f = 514$ Hz, is 1.125 W. As the coaxial air to fuel jet velocity ratio was increased during forcing of coaxial air into the fuel jet, the flame length was reduced by up to $80d_f$, which is about 45% of $L_{f,0}$ ($= 180d_f$), where $L_{f,0}$ indicates the flame length of simple jet flames without coaxial air [1]. This reduction is explained by the fact that coaxial air induces increased mixing of fuel and air. Moreover, when there is additional forcing of coaxial air into the fuel jet, the flame length is further reduced compared to that of a flame without acoustic excitation. Quantitatively, a 15% reduction in flame length was achieved in coaxial jet flames with acoustic excitation. This additional reduction is thought to be caused by enhanced mixing due to large vortical motions formed in the outer mixing layer.

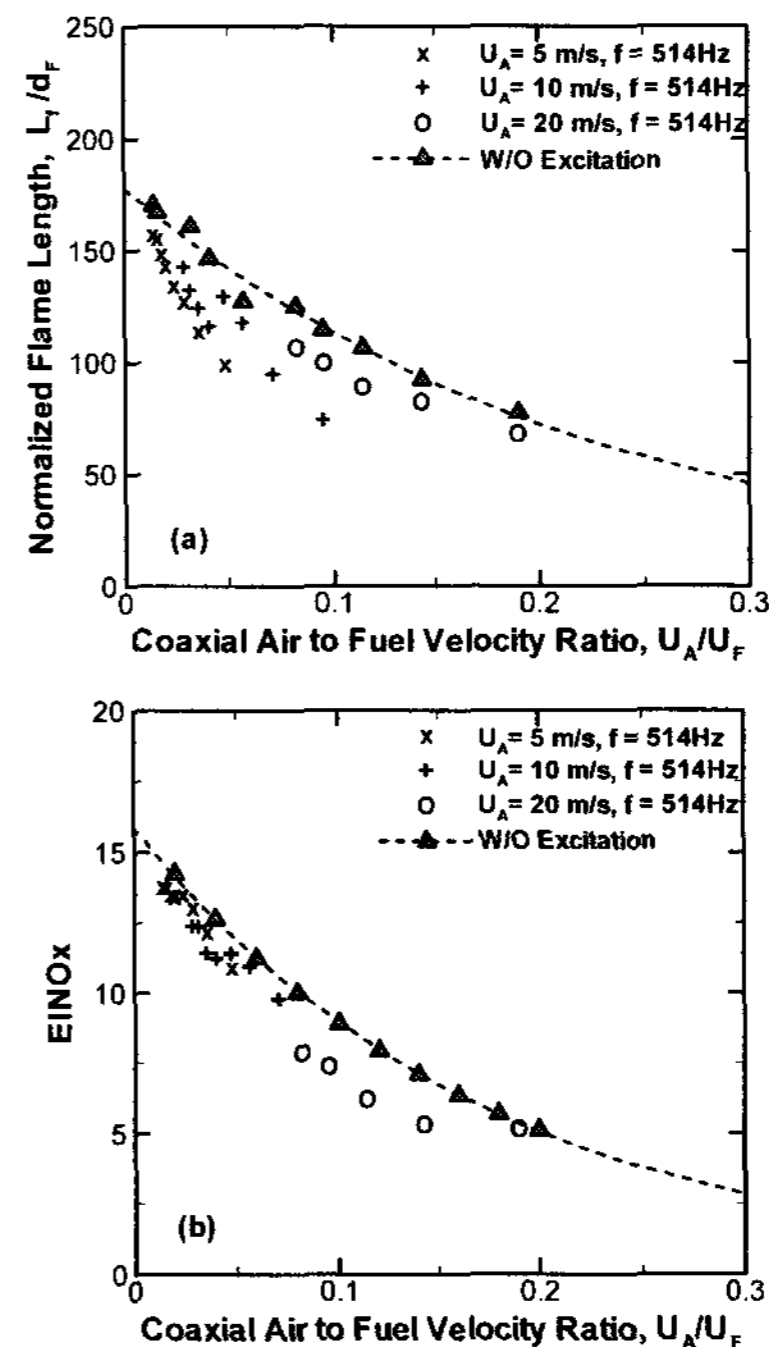


Figure 2. (a) Normalized flame length and (b) EINOx variation in coaxial air flames with and without acoustic excitation at 514 Hz with $P=1.125$ W. Symbols 'x', '+', and 'o' means $U_A=5$, 10, and 20 m/s respectively, with increasing U_F with excitation. The dashed line indicates the cases without excitation.

To find the effect of acoustic excitation on NOx emission, NOx measurements were also performed on coaxial jet flames with acoustic excitation at $f = 514$ Hz and $P = 1.125$ W, and compared to coaxial jet flames without acoustic excitation. In Fig. 2(b), EINOx data show a similar trend to the normalized flame length data. With increasing coaxial air to fuel velocity ratio, coaxial air efficiently decreased EINOx levels and EINOx levels were decreased even further with acoustic excitation. For instance, the value of EINOx was 17.0 for simple jet flames of $U_F = 175$ m/s and decreased to as little as 8.2 when coaxial air of $U_A=20$ m/s was added into the fuel jet. When acoustic forcing was also used to mix coaxial air and fuel, EINOx was further reduced to as little as 6.2, which means that a total 64 % reduction in EINOx was achieved eventually. This additional decrease in flame length and EINOx by acoustic excitation is closely related to mixing enhancement in the near field, where a streamwise vortex plays an important role.

3.2 Flame/Vortex Interactions

3.2.1 Mean Velocities at the Flame Surface

From PIV and OH PLIF measurement, flow properties at the flame surface can be determined, such as mean axial velocity, u_x , and mean radial velocity, u_r . The flame surface is approximated by the OH layer. Figure 3(a) shows the phase-lock averaged velocity field

overlapped by the phase-lock averaged OH layer for the case of $U_F = 175$ m/s and $U_A = 10$ m/s at $f = 514$ Hz and $P = 1.125$ W. The phase was locked at $\phi = 0^\circ$. The contour indicates the distribution of the mean axial velocity. The mean axial velocity, u_x varies as the vortex pair rolls up and goes downstream. Accordingly, the high u_x region coincides with the region of the vortex rollup.

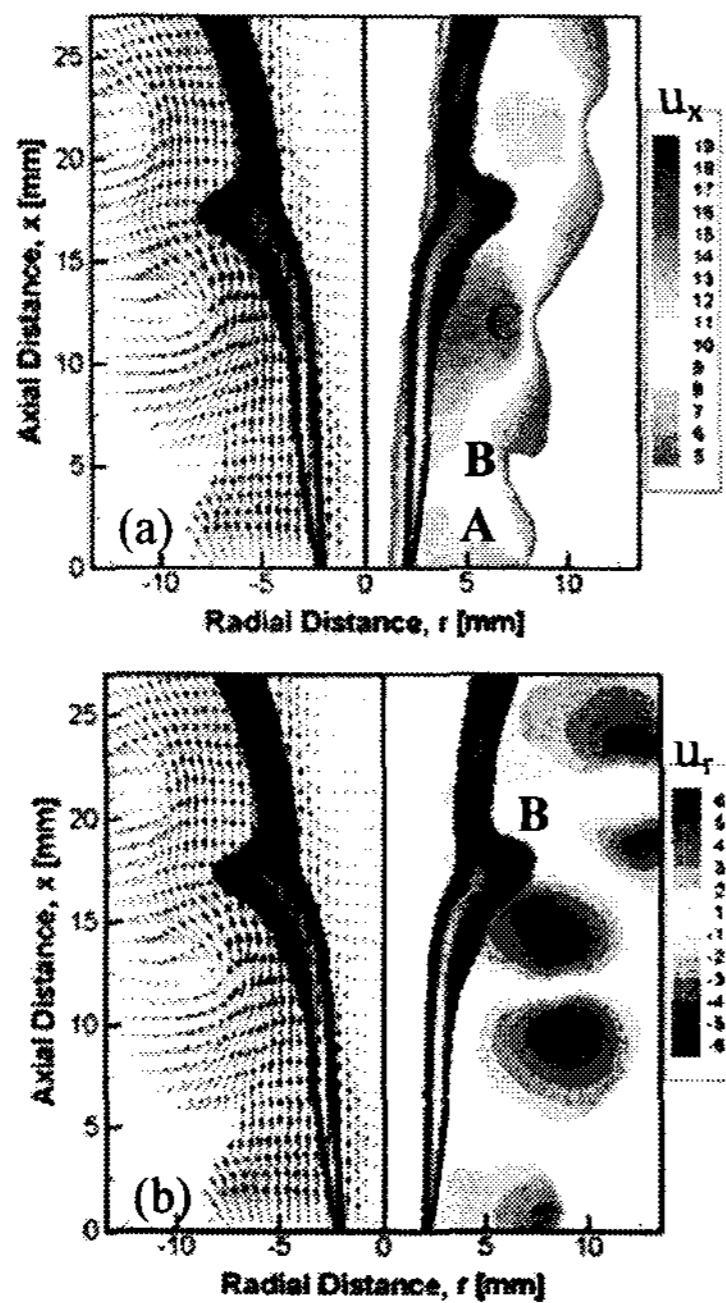


Figure 3. Phase-lock averaged velocity vectors and contours overlapped by the OH layer. The right-hand contour indicates (a) axial mean velocity, u_x and (b) radial mean velocity, u_r , respectively.

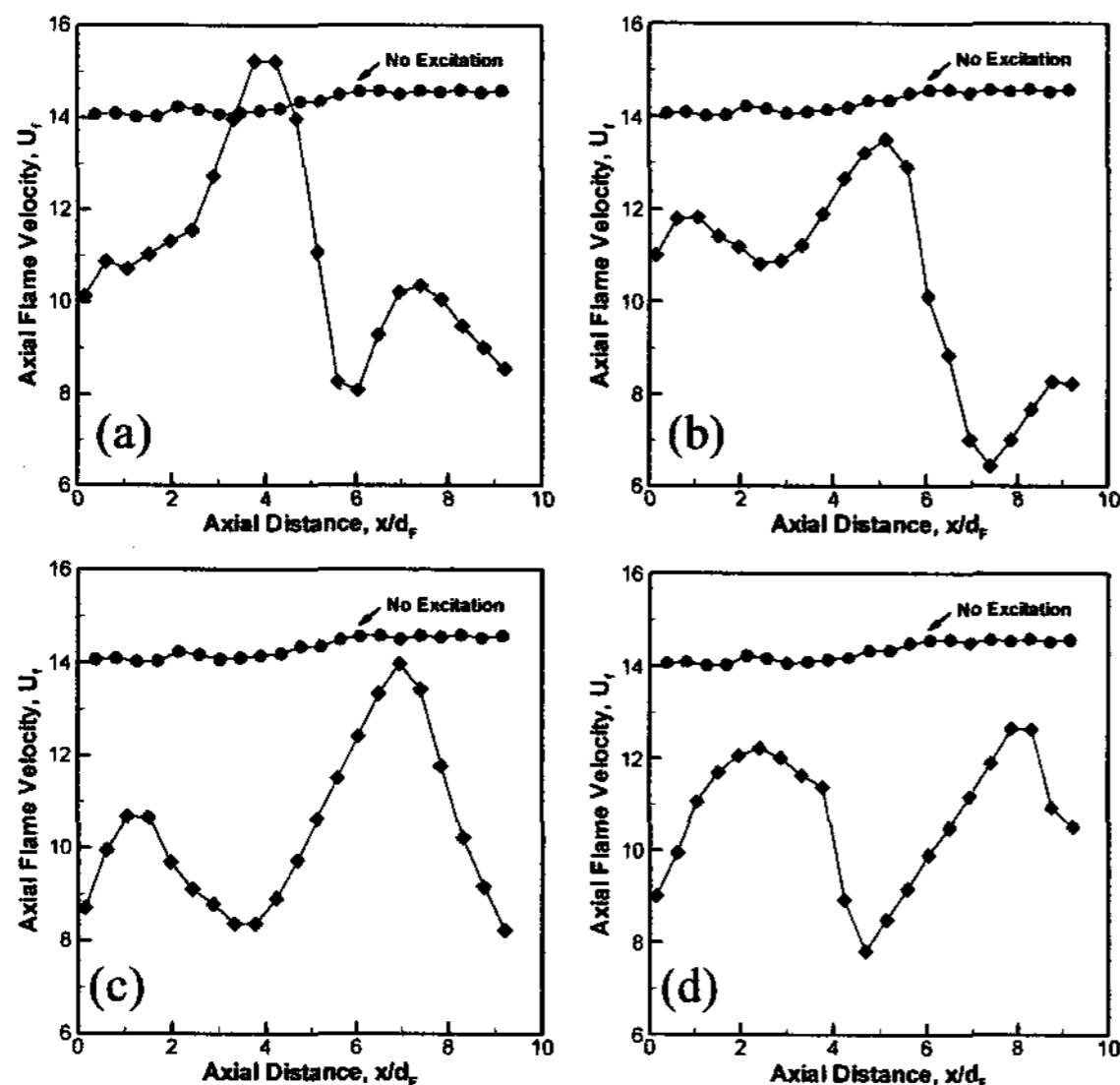


Figure 4. Variation of U_f along the axial distance in the flame of $U_F=175$ m/s and $U_A=10$ m/s at $f=514$ Hz and $P=1.125$ W. The phase is locked at (a) $\phi=0^\circ$, (b) $\phi=90^\circ$, (c) $\phi=180^\circ$ and (d) $\phi=270^\circ$.

Along the OH layer, we can extract the mean axial velocity, U_f . U_f is representative of the mean axial velocity at the flame surface. The result of U_f at $\phi = 0^\circ$ is presented in Fig. 4(a). For the flame without acoustic excitation, U_f is nearly constant (~ 14 m/s) along the downstream direction. But, in the flame with acoustic forcing, U_f fluctuates from 'A' to 'C', along the axial distance because coaxial air velocity oscillates with acoustic pulsing.

As the phase is varied from $\phi = 90^\circ$ to $\phi = 270^\circ$, the variations in the axial velocity at the flame surface, U_f , are shown in Fig. 4(b)-(d). As the phase is increased, U_f of region 'A' increases and after one cycle of phase angle, U_f increases beyond the value of the case without acoustic excitation, shown in 'C' of Fig. 4(a). This velocity fluctuation of U_f repeatedly moves downstream as the cycle of the signal.

Along the OH layer, the mean radial velocity, u_r on the flame surface can be determined. As shown in Fig. 5, u_r is less than 1 m/s for all axial location for the flame of $U_F = 175$ m/s and $U_A = 10$ m/s without acoustic excitation. If the flame surface is tilted against the x -axis, however, u_r does not indicate the velocity entrained into the flame surface. As illustrated in Fig. 6, the tilted angle of the flame sheet is given by θ . The entrainment velocity on the flame surface can then be defined as:

$$u_E = u_r \cos \theta + U_f \sin \theta \quad (1)$$

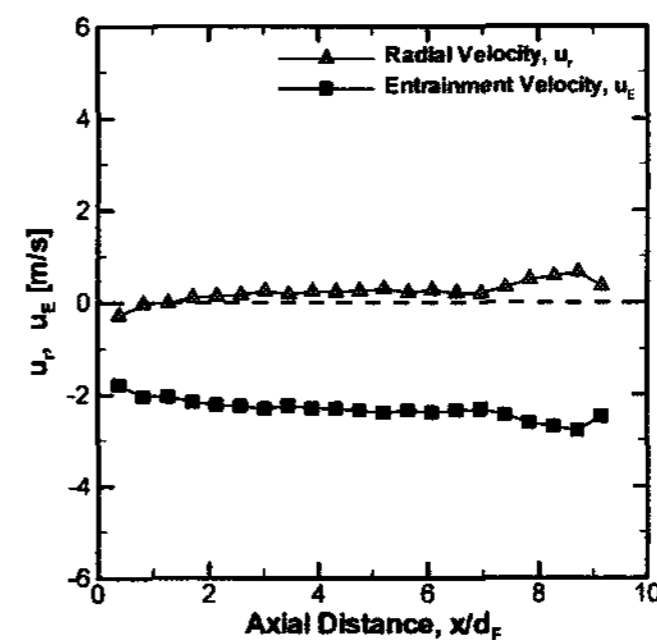


Fig.5 Variations of u_r and u_E along the axial distance in the flame of $U_F=175$ m/s and $U_A=10$ m/s without acoustic excitation.

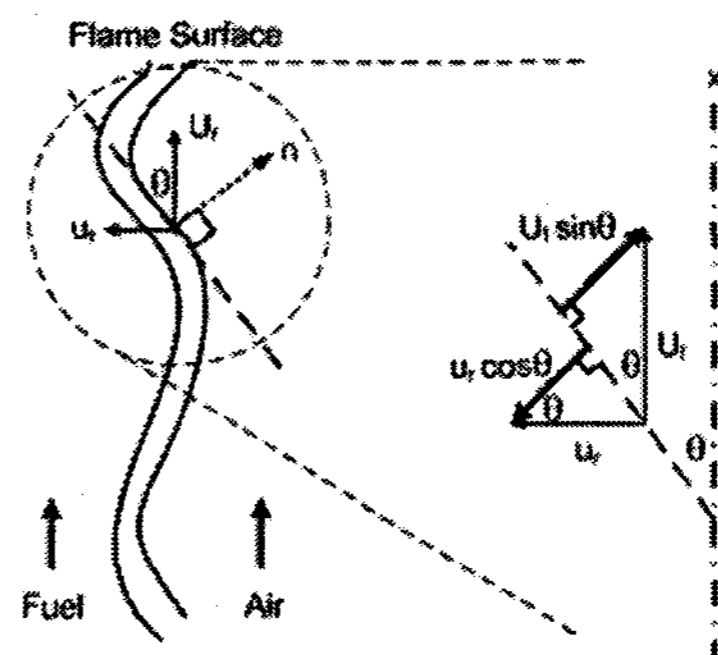


Figure 6. Geometric parameters and definitions required to calculate entrainment velocity, u_E .

where the tilted angle, θ , is calculated from the OH layer.

The result for u_E is presented in Fig. 5. The value of u_E is about 2 m/s, which is larger than u_r but has negative sign. By definition, a negative velocity represents a velocity directing radially into the flame surface and a positive velocity is a velocity directing radially outward from the flame surface.

Figure 3(b) shows the phase-lock averaged velocity field overlapped by the OH layer for the flame of $U_F = 175$ m/s and $U_A = 10$ m/s at $f = 514$ Hz and $P = 1.125$ W. The phase was locked at $\phi = 0^\circ$. The contour represents the distribution of the mean radial velocity. Along the vertical axis, centered at the vortex core, the mean radial velocity changes from negative to positive due to the vortex motion. In Fig. 7(a), the mean radial velocity, u_r , and the entrainment velocity, u_E , are obtained along the OH layer. Since the flame surface is stretched by the large-scale vortical motion, u_E increases up to 6 m/s at region 'A' near the vortex. In contrast, u_E decreases drastically and becomes negative at region 'B'. This means that vortex interaction with the flame enhances the mixing rate of air and fuel.

Similarly, the results of u_r and u_E according to the phase angle of the acoustic signal are shown in Fig. 7(b)-(d). It is found that entrainment velocity increases along the axial distance and, after a certain axial location, it appears to decrease gradually due to viscous decay of the vortex. Therefore, we can conclude that the large-scale coherent vortex generated by acoustic forcing plays a dominant role in enhanced mixing of fuel and air in the near field.

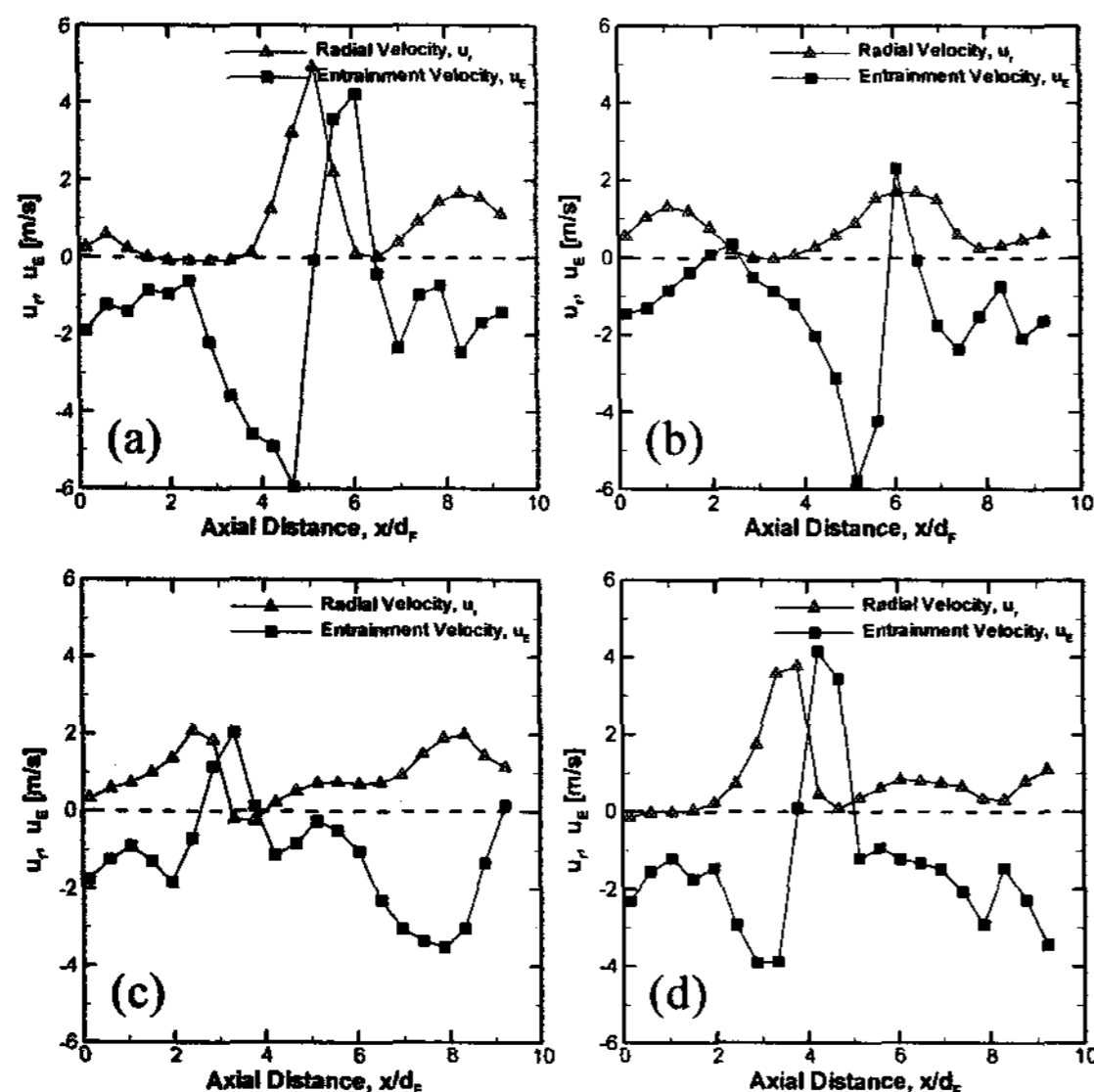


Figure 7. Variations of u_r and u_E along the axial distance in the flame of $U_F = 175$ m/s and $U_A = 10$ m/s at $f = 514$ Hz and $P = 1.125$ W. The phase is locked at (a) $\phi = 0^\circ$, (b) $\phi = 90^\circ$, (c) $\phi = 180^\circ$ and (d) $\phi = 270^\circ$.

3.2.2 Flame Surface Area

The averaged OH PLIF image was obtained from one hundred instantaneous images. For flame without acoustic excitation, the flame width became broader with increasing axial distance. The flame width is affected by the large-scale vortical motion. That is, the flame sheet is stretched radially toward the coaxial air jet. To confirm this qualitative inference, the approximated flame surface area, A_f , can be calculated by integration of the OH layer, which is an indicator used to identify the flame front in hydrogen/air jet flames. Figure 8 indicates that A_f was about 519.09 mm² for the flame without acoustic excitation. But, under acoustic forcing, the flame surface area, A_f is significantly increased up to about 600 mm², which is 15% larger than without acoustic excitation. This increase in flame surface area and entrainment velocity is a crucial factor in reducing flame length and NOx emission in coaxial jet flames with acoustic excitation.

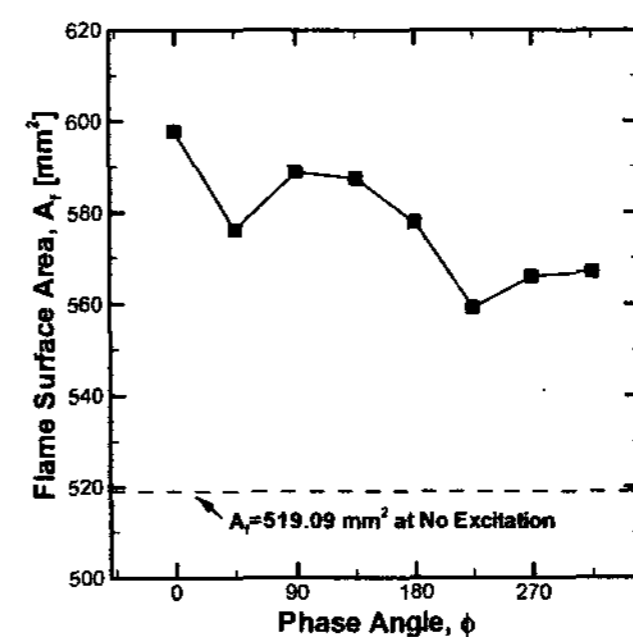


Figure 8. Variations of approximated flame surface area according the phase angle in the flame of $U_F = 175$ m/s and $U_A = 10$ m/s with acoustic excitation at $f = 514$ Hz, $P = 1.125$ W.

4. Conclusion

Experimental measurements of NOx, velocity field and concentration field were conducted in order to investigate dynamic behaviors in the near field of turbulent hydrogen nonpremixed flames by acoustically generated resonant coaxial air. A resonance frequency was selected for acoustic forcing of the coaxial air because of its ability to effectively amplify acoustic amplitude and reduce NOx emissions. When acoustic pulsing at the resonance frequency is imposed, a streamwise vortex is formed in the outer mixing layer of the coaxial air jet. Acoustic excitation causes velocity fluctuations of the coaxial air jet as well as of the fuel jet. The vortex, which is periodically generated by acoustic excitation, enhances the mixing rate of fuel and air, thus the normalized flame length is reduced by 15% and consequently, a 25 % reduction in EINOx is achieved

compared to a flame without acoustic excitation.

From phase-lock PIV/OH PLIF images, we analysed mean velocity information at the flame surface according to the phase of the signal. The mean axial velocity at the flame surface fluctuates up and down along the axial distance because the flame surface is affected by vortex roll-up. This fluctuation of the mean axial velocity goes downstream as the phase is increased. Accounting for the tilted angle of the flame surface, the entrainment velocity can be extracted from the mean radial velocity at the flame surface. The entrainment velocity is considerably increased near the flame surface outwardly stretched by the vortex. From integration of the averaged OH image, we found that the approximated flame surface area is increased significantly under acoustic forcing. This increase in entrainment velocity and flame surface area is a crucial factor in reducing flame length and NO_x emission in coaxial jet flames with acoustic excitation. Finally, we observed that local flame extinction occurs frequently because of excessive influx of fuel and entrained air.

- 9) Demare, D. and Baillot, F., 2004, "Acoustic Enhancement of Combustion in Lifted Nonpremixed Jet Flames," *Combust. Flame*, Vol.139, pp.312~328.

References

- 1) Chen, R. H. and Driscoll, J. F., 1990, "Nitric Oxide Levels of Jet Diffusion Flames: Effects of Coaxial Air and Other Mixing Parameters," *Proc. Combust. Inst.*, Vol.23, pp.281~288.
- 2) Kim, S. H., Yoon, Y. and Jeung, I.S., 2000, "Nitrogen Oxides Emissions in Turbulent Hydrogen Jet Non-Premixed Flames: Effects of Coaxial Air and Flame Radiation," *Proc. Combust. Inst.*, Vol.28, pp.463~471.
- 3) Renard, P. -H., Thévenin, D., Rolon, J. C. and Candel, S., 2000, "Dynamics of Flame/Vortex Interactions," *Prog. Ener. Combust. Sci.*, Vol.26, pp.225~282.
- 4) Mueller, C. J. and Schefer, R. W., 1998, "Coupling of Diffusion Flame Structure to an Unsteady Vortical Flow-Field," *Proc. Combust. Inst.*, Vol.27, pp.1105~1112.
- 5) Takahashi, F., Schmoll, W. J., Trump, D. D. and Goss, L. P., 1996, "Vortex-Flame Interactions and Extinction in Turbulent Jet Diffusion Flames," *Proc. Combust. Inst.*, Vol.26, pp.145~152.
- 6) Zheng, X. L., Yuan, J. and Law, C. K., 2004, "Nonpremixed Ignition of H₂/Air in a Mixing Layer with a Vortex," *Proc. Combust. Inst.*, Vol.30, pp.415~421.
- 7) Chao, Y. -C., Yuan, T. and Tseng, C. -S., 1996, "Effects of Flame Lifting and Acoustic Excitation on the Reduction of NO_x Emissions," *Combust. Sci. Technol.*, Vol.113-114, pp.49~65.
- 8) Parr, T. P., Gutmark, E., Wilson, K., Hanson-Parr, D. M., Yu, K., Smith, R. A. and Schadow, K. C., 1996, "Compact Incinerator Afterburner Concept Based on Vortex Combustion," *Proc. Combust. Inst.*, Vol.26, pp.2471~2477.